

# A Microfluidic Platform for Evaporation-based Salt Screening of Pharmaceutical Parent compounds

*Sachit Goyal<sup>a</sup>, Michael R. Thorson<sup>a</sup>, Cassandra L. Schneider<sup>a</sup>, Geoff G.Z. Zhang<sup>b</sup>, Yuchuan Gong<sup>b</sup>,  
and Paul J.A. Kenis<sup>a</sup>*

## Supplementary Information

### 1. *Fabrication procedure for the three-layer assembly (TLA)*

Negative patterns of SU-8 2050 (MicroChem) photoresist were patterned on to silicon wafers (University wafer) to a thickness of 50  $\mu\text{m}$  for the fluid layer and control layer masters using standard photolithography. The master molds were silanized with a monolayer of tridecafluoro-1,1,2,2-tetrahydrooctyl trichlorosilane (Gelest) to prevent covalent adhesion of PDMS to the silicon substrates. The thickness of photoresist and PDMS layers were verified using a surface profilometer (Dektak 3030). Control layers (80  $\mu\text{m}$ ) and fluid layers (70  $\mu\text{m}$ ) were obtained by spin coating (G3P-8 Spin Coat by Specialty Coating Systems) 5:1 A:B, PDMS and 15:1 A:B, PDMS at 1100 and 1200 rpm, respectively. The control layer and the fluid layer were partially cured on a digital hot plate / stirrer (Dataplate<sup>®</sup> 730 series, Barnstead Thermolyne) at 80°C for approximately 5 and 15 minutes respectively. Next, a 2mil (50  $\mu\text{m}$ ) COC sheet was bonded irreversibly to the top of the control layer mold after treatment with oxygen plasma in plasma cleaner (Harrick Plasma) for 1 minute. The COC-control layer assembly was then heated at 80°C for 10 minutes on a hot plate. Next, the COC-control layer assembly was carefully lifted off the control layer master. The embossed side of the PDMS control layer was covered with Scotch<sup>™</sup> removable tape (3M) following which through holes were drilled (Dremel 300 series drill with a 750  $\mu\text{m}$  McMaster-Carr drill bit) to create inlets for vacuum actuation. Next, the control layer was manually aligned and placed on the fluid layer under an optical microscope (Leica MZ6), followed by heating at 80°C for 20–30 minutes on a hot plate to bond the layers. After lifting the three-layer assembly off the fluid layer master, the fluid layer side was covered with Scotch<sup>™</sup> removable tape (3M). Through-holes were drilled at the fluid layer inlets and outlets. Subsequently, a 3 to 5 mm thick PDMS layer (5:1 A:B) was irreversibly bonded to the top of the three-layer assembly covering the fluid layer and the control layer inlets, after treatment with an oxygen plasma for 1 minute. Through-holes were punched into the thick PDMS layer with a 20-gauge needle (BD PrecisionGlide<sup>™</sup>) through the holes already drilled at the control layer and the fluid layer inlets.

## 2. Assembly and Dis-assembly of the Microfluidic Platform

Assembly of different layers (TLA-IL-EL) for setting up of the crystallization screening experiment is shown in Fig. S1. The IL is aligned onto the thiolene EL after holes corresponding to those in the EL are drilled into the IL using a 100  $\mu\text{m}$  drill bit (McMaster). The burrs are removed from the holes using a scalpel to ensure flat IL and absence of air pockets between IL and EL. The TLA is then aligned on to the IL-EL assembly. At the end of the crystallization experiment the TLA-IL assembly is lifted off from the EL. The TLA-IL assembly is then used for further analyses of the solid forms using on-chip birefringence analysis and Raman analysis. The EL can be reused for other experiments.

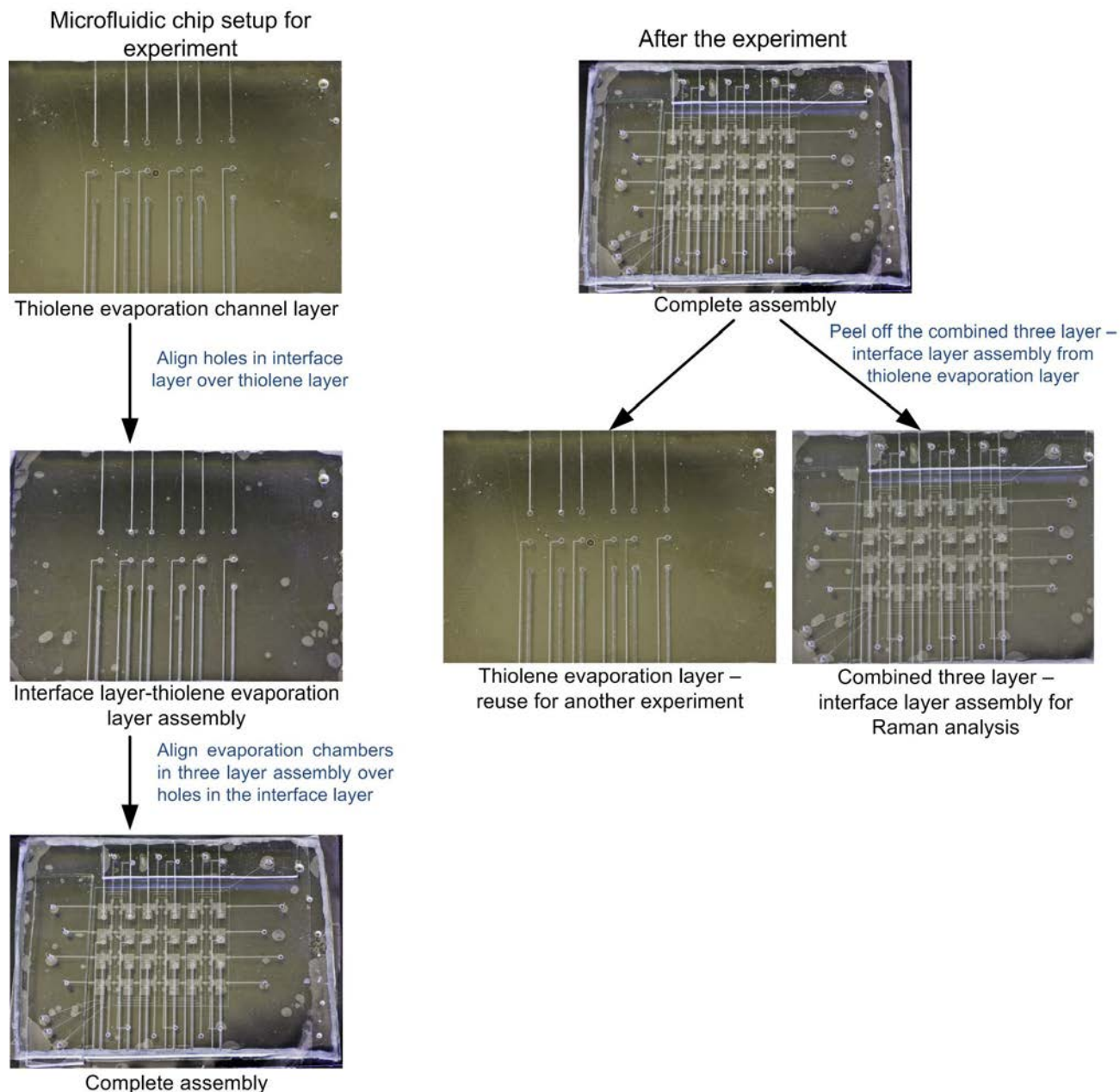


**Fig. S1** Procedure showing (a) assembly the chip for conducting an evaporation experiment, (b) dis-assembly the chip after the experiment to carry out on-chip birefringence and Raman analysis and re-use the thiolene evaporation channel layer.

Fig. S2 shows the tiled optical micrograph of the complete chip (TLA-IL-EL assembly) for an on-chip screen of salt solid forms of ephedrine. The evaporation channels in the EL are highlighted. Three different rates of evaporation were induced externally labeled as A (row 1), B (row 2), and C (row 3). The last row corresponds to control where solvent loss results from materials comprising the chip.

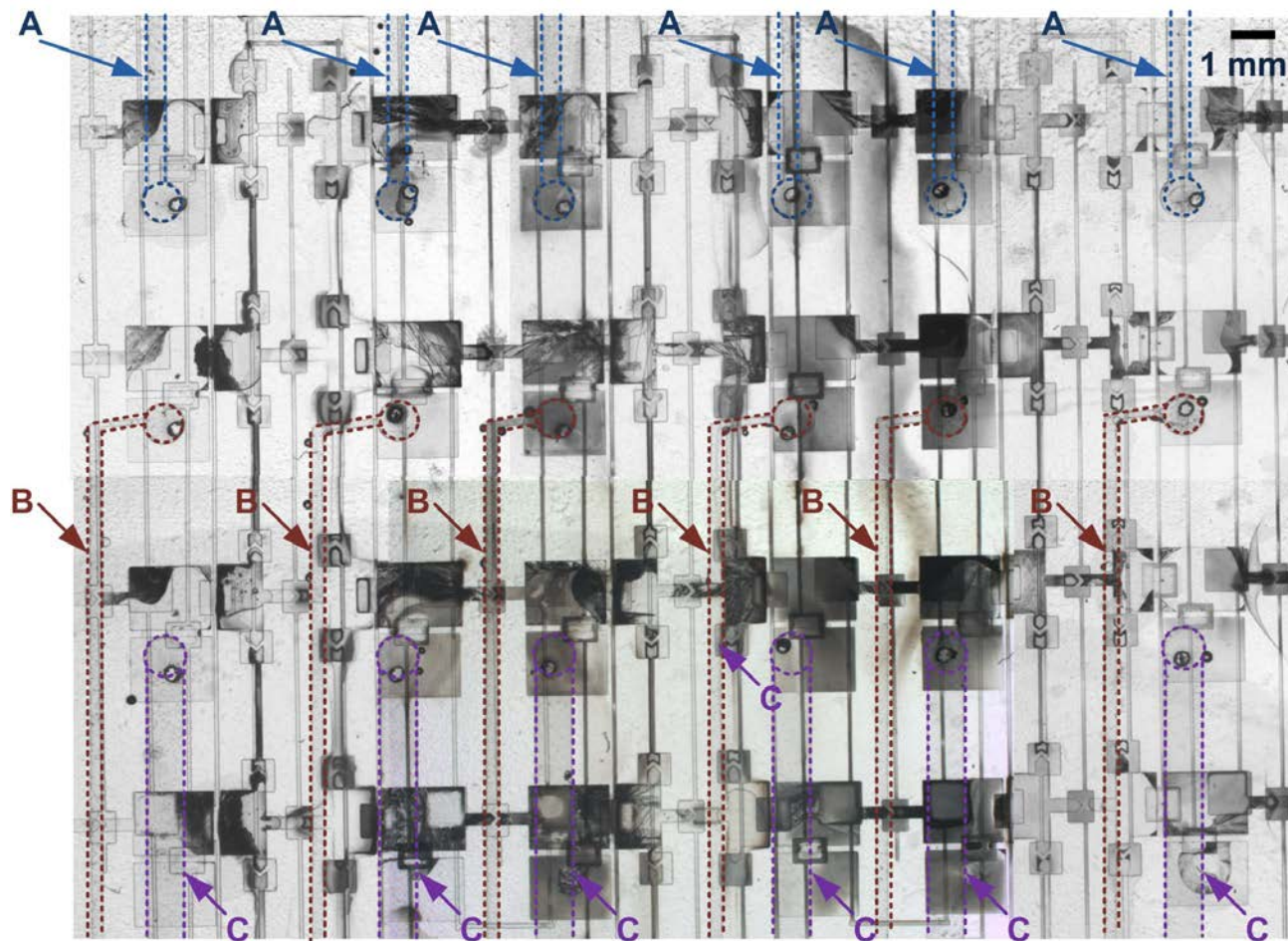


**Fig. S2** Tiled optical micrographs for an on-chip screen of salt solid forms of ephedrine, with the three-layer assembly, the interfacial layer, and the evaporation channel layer assembled together. The different dimension evaporation channels (A, B, and C) are highlighted.

### 3. Solvent Evaporation Rate Plots for Different Solvents Attained On-Chip

Solvent evaporation was quantified as a function of time for two different solvents: water and methanol by tracing the area covered by the solvent in the microfluidic crystallization well using the “freehand selection” tool in ImageJ 1.46. Fig. S3 shows representative solvent evaporation plots (in percentage volume of the solvent) for methanol (Fig. S3a) and water (Fig. S3b). We observed that the solvents evaporation rates were indeed at different rates as shown by the trends. The solvent loss was observed to be a combination of solvent loss resulting from chip material (TLA-IL assembly) and the solvent evaporation through the microchannels in the EL connecting the liquid to the ambient conditions. In the case of evaporation of methanol, control experiment resulted in evaporation rate of ~4 nL/hr, and different evaporation channels adjusted for control (assuming additive effect) were 3, 6, and 12 nL/hr corresponding to as expected evaporation rates of about 3.75, 7.5, and 15 nL/hr, respectively. The evaporation rates in the case of water as solvent were very low due to low volatility of water and minimal solvent loss through chip material compared to alcohols such as methanol. Table S1 shows the dimensions of the evaporation channels corresponding to different solvent evaporation rates (computed analytically).

**Table S1** Dimensions of the evaporation channels in the EL

		Evaporation channel layer dimensions				
		Length (cm)	Width ( $\mu\text{m}$ )	Height ( $\mu\text{m}$ )	Area of cross-section ( $A_c$ ) ( $\mu\text{m}^2$ )	$A_c/L$ ( $\mu\text{m}$ )
Rate of solvent evaporation (nL/hr)	3.75	2.5	150	100	15000	0.6
	7.5	1.8	220	100	22000	~1.2
	15	1.8	440	100	44000	~2.4

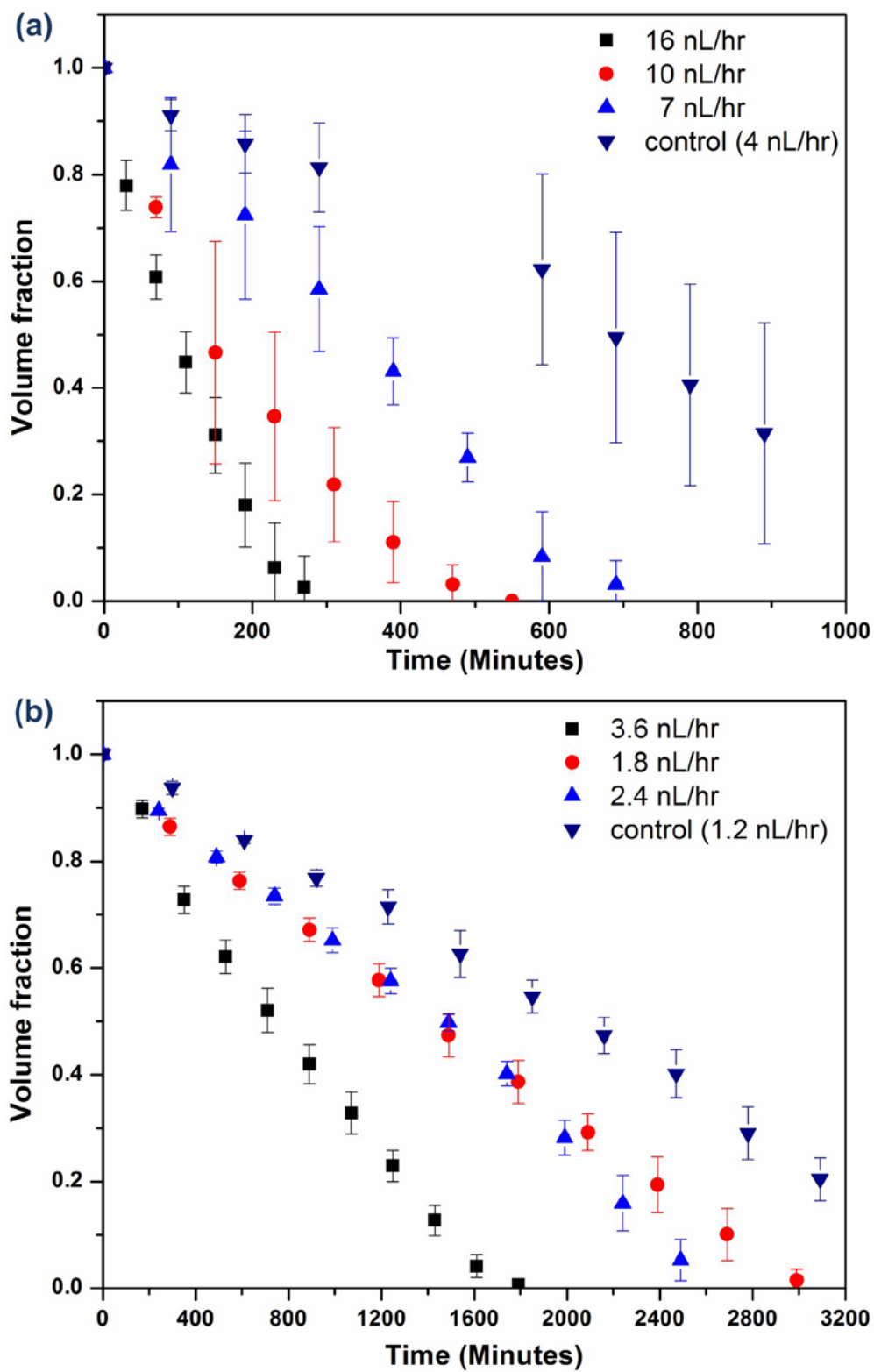


**Fig. S3** Graphs showing (a) evaporation of alcohols on-chip (methanol) and (b) evaporation of water on-chip as a function of time. The legends correspond to the actual evaporation rate computed by fitting a straight line for each trend.

#### 4. Raman Spectra for Materials Comprising the Microfluidic Chip and an Empty Chip

The Raman spectra for different materials that the TLA-IL assembly comprises of *i.e.* polydimethylsiloxane (PDMS) and cyclic olefin copolymer (COC), and for an assembled empty chip (Empty chip refers to TLA-IL assembly of the microfluidic platform) are provided in Fig. S4. Acquisition of individual Raman spectrum for different materials the TLA-IL assembly is comprised of helps in analyzing the individual contributions of different materials to the peaks in the spectrum for the empty microfluidic chip. From Figure S3, we can infer that the peaks in the spectrum for empty chips are mainly due to PDMS, whereas there is minimum contribution due to COC.

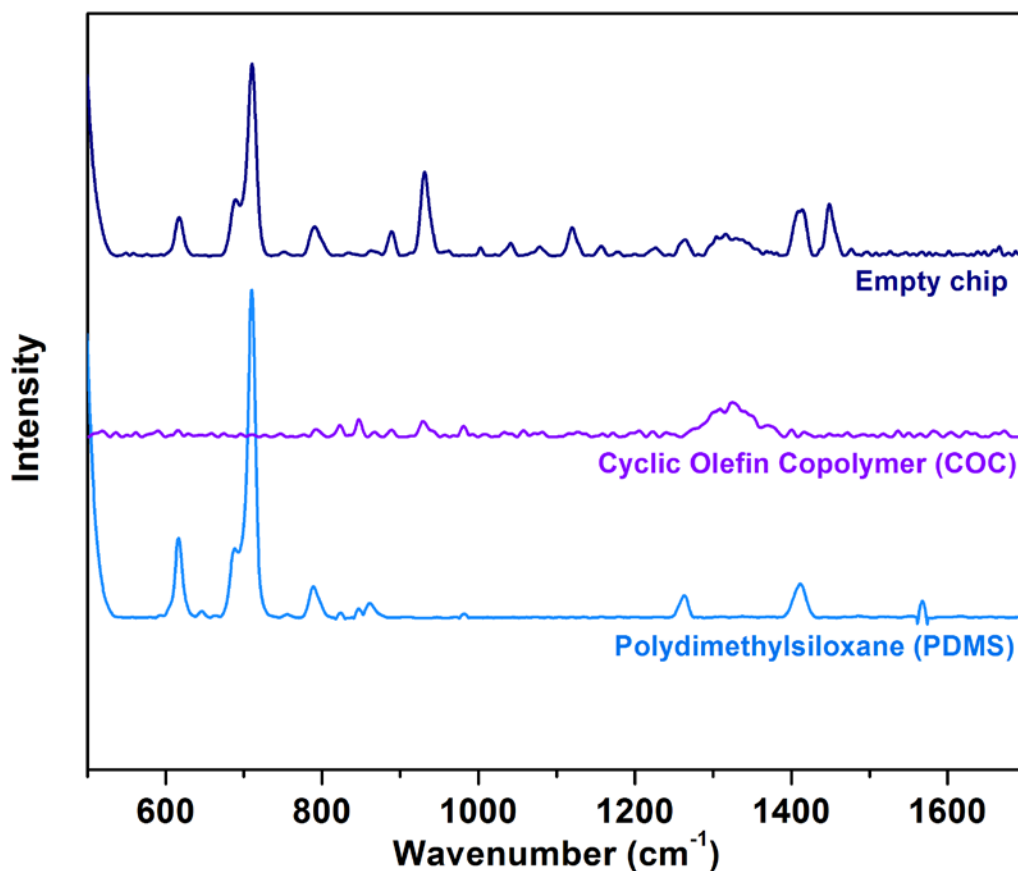


**Fig. S4** Raman spectroscopy data for empty chip corresponding to the three layer – interface layer assembly, polydimethylsiloxane (PDMS), and cyclic olefin copolymer (COC). The microfluidic platform is comprised of PDMS and COC layers.

## **5. Correcting On-chip Raman Spectrum for Background from Empty Microfluidic Chip**

The following procedure is followed to verify the identity of the solid forms crystallized on-chip. The Raman spectra for each solid form crystallized on-chip and the “empty microfluidic platform” (TLA-IL assembly) are obtained. The Raman spectrum of the solid form obtained on-chip is then corrected for the spectrum for the empty microfluidic platform. The background from the empty chip was not significant compared to the Raman spectrum for solid forms crystallized on-chip, hence on correction only the peaks pertaining to the empty chip were removed from the Raman spectrum of the solid forms crystallized on-chip. The corrected Raman spectrum of the solid form crystallized on-chip is then compared to the Raman spectrum of PC, of the corresponding salt form crystallized in an off-chip experiment, and of the corresponding salt former to verify the identity of the solid form crystallized on-chip. Figure S4 shows on-chip Raman data acquisition, background correction, and comparison of the Raman spectra of on-chip and off-chip grown crystals for ephedrine esylate (Fig. S5a) and tamoxifen citrate (Fig. S5b). The background corrected Raman spectra for ephedrine esylate and tamoxifen citrate crystallized on-chip were in good agreement with the spectra of the respective salt forms crystallized in an off-chip experiment, and was significantly different from the Raman spectra for pure PC's and the corresponding salt formers. This validated the formation of salt forms on-chip.

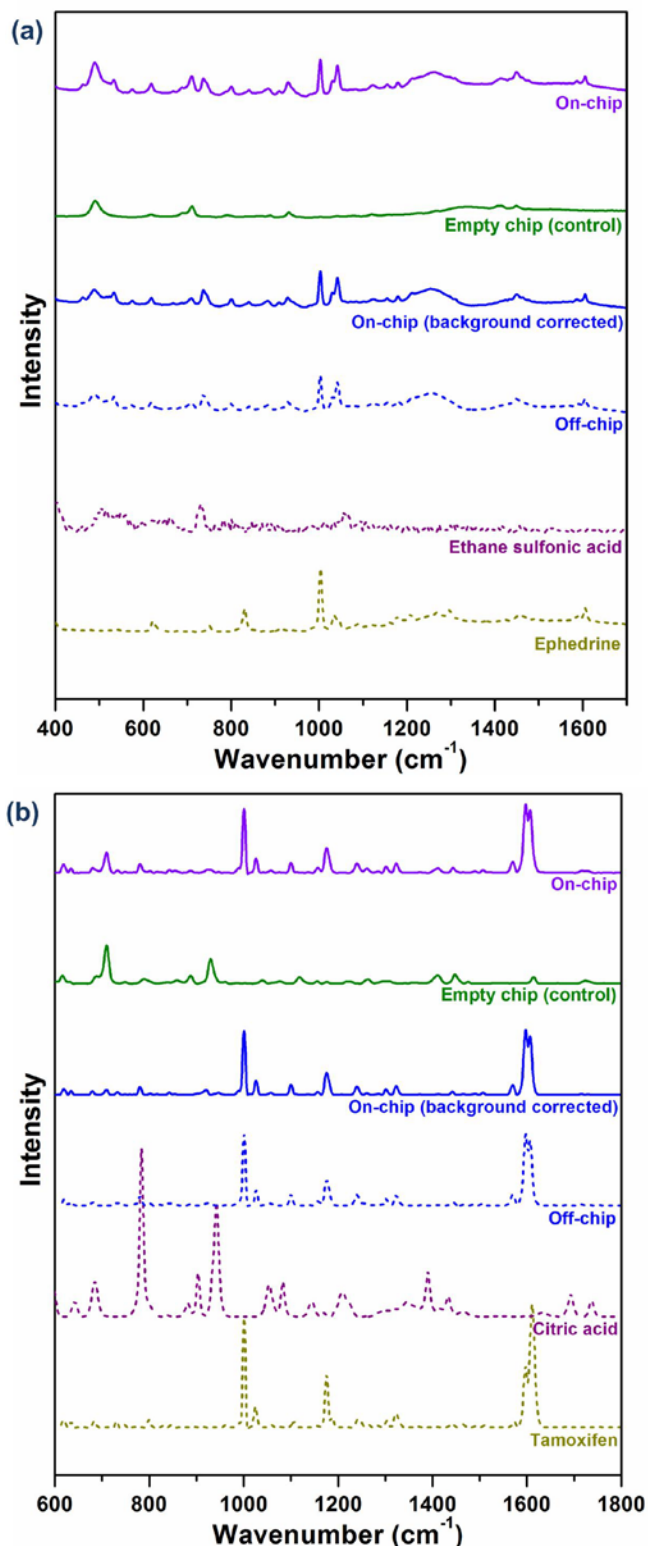


**Fig. S5** Raman spectroscopy data of (a) ephedrine esylate salt crystallized on-chip and off-chip, “empty microfluidic chip” corresponding to the TLA-IL assembly, ephedrine esylate crystallized on-chip (corrected for empty chip background), ethane sulfonic acid (off-chip), and ephedrine (off-chip) and (b) tamoxifen citrate salt crystallized on-chip and off-chip, empty microfluidic chip corresponding to the three layer – interface layer assembly, tamoxifen citrate crystallized on-chip (corrected for empty chip background), citric acid (off-chip), and tamoxifen (off-chip). The off-chip crystals of the salt forms were grown in 1 mL glass vials.